Title

Stepwise processing analyses of the single-turnover PCSK9 protease reveal its substrate sequence specificity and link clinical genotype to lipid phenotype

Journal

Journal of Biological Chemistry, 293(6)

ISSN

0021-9258

Authors

Chorba, John S
Galvan, Adri M
Shokat, Kevan M

Publication Date

2018-02-01

DOI

10.1074/jbc.ra117.000754

Stepwise processing analyses of the single-turnover PCSK9 protease reveal its substrate sequence specificity and link clinical genotype to lipid phenotype

Received for publication, November 1, 2017, and in revised form, December 10, 2017 Published, Papers in Press, December 19, 2017, DOI 10.1074/jbc.RA117.000754

John S. Chorba[‡§1], **Adri M. Galvan**[§], **and Kevan M. Shokat**[§]

From the [‡]*Division of Cardiology, Department of Medicine, Zuckerberg San Francisco General and University of California, San Francisco, California 94110 and the* [§]*Department of Cellular and Molecular Pharmacology and Howard Hughes Medical Institute, University of California, San Francisco, California 94143*

Edited by George N. DeMartino

Proprotein convertase subtilisin/kexin type 9 (PCSK9) downregulates the low-density lipoprotein (LDL) receptor, elevating LDL cholesterol and accelerating atherosclerotic heart disease, making it a promising cardiovascular drug target. To achieve its maximal effect on the LDL receptor, PCSK9 requires autoproteolysis. After cleavage, PCSK9 retains its prodomain in the active site as a self-inhibitor. Unlike other proprotein convertases, however, this retention is permanent, inhibiting any further protease activity for the remainder of its life cycle. Such inhibition has proven a major challenge toward a complete biochemical characterization of PCSK9's proteolytic function, which could inform therapeutic approaches against its hypercholesterolemic effects. To address this challenge, we employed a cell-based, high-throughput method using a luciferase readout to evaluate the single-turnover PCSK9 proteolytic event. We combined this method with saturation mutagenesis libraries to interrogate the sequence specificities of PCSK9 cleavage and proteolysis-independent secretion. Our results highlight several key differences in sequence identity between these two steps, complement known structural data, and suggest that PCSK9 self-proteolysis is the rate-limiting step of secretion. Additionally, we found that for missense SNPs within PCSK9, alterations in both proteolysis and secretion are common. Last, we show that some SNPs allosterically modulate PCSK9's substrate sequence specificity. Our findings indicate that PCSK9 proteolysis acts as a commonly perturbed but critical switch in controlling lipid homeostasis and provide a new hope for the development of small-molecule PCSK9 inhibitors.

On the cell surface of the hepatocyte, proprotein convertase subtilisin/kexin type 9 (PCSK9)[2] binds to the LDL receptor (LDL-R) and, upon internalization, chaperones the entire complex to the lysosome for degradation (1, 2). By preventing recycling of the LDL-R back to the cell surface, PCSK9 reduces the availability of the LDL-R to remove LDL cholesterol (LDL-C) from the bloodstream (3, 4), which ultimately promotes atherosclerotic heart disease (5, 6). Therapeutics targeting PCSK9 function lead to impressive reductions in LDL-C in patients and, for those with established heart disease, provide additional clinical benefit beyond standard therapy (7, 8). The large therapeutic window of PCSK9 inhibition along with the prevalence of the underlying disease justify a need for additional anti-PCSK9 therapies, particularly ones amenable to lower manufacturing costs or oral administration, such as small molecules.

Successful processing of the PCSK9 polypeptide is required for its maximal effect on the LDL-R (9). PCSK9 contains a signal sequence to direct its translation to the ER, where it then folds into a self-cleaving zymogen (10). Like other proprotein convertases, self-cleavage of the prodomain is required for PCSK9 to exit the ER, transit the secretory pathway, and reach the extracellular space (11). Unlike other proprotein convertases, however, PCSK9 does not cleave its prodomain a second time. Instead, the prodomain C terminus remains bound in the active site, inhibiting further proteolytic function (12). Disruption of PCSK9 proteolysis is an attractive strategy to inhibit PCSK9 function, particularly as genetic variants within the cleavage sequence preventing autoproteolysis protect against cardiovascular disease (13). Unfortunately, the self-inhibition of PCSK9 has proven to be a major challenge toward a complete biochemical characterization of its proteolytic activity. Furthermore, although the structure of mature PCSK9 has been solved by multiple groups (12, 14, 15), no structure of the uncleaved proPCSK9 has been reported.

In this work, we approach these challenges by developing a luciferase-based assay to evaluate PCSK9 proteolytic activity in *trans*. We use this assay to characterize the protease sequence specificity, which correlates with known structural data of the

This work was supported by NHLBI, National Institutes of Health (NIH), Grants K08 HL124068 and LRP HMOT1243; NCATS, NIH, through the University of California San Francisco Clinical and Translational Science Institute Catalyst Program (Grant UL1 TR000004); the University of California San Francisco Academic Senate; the Hellman Foundation; a Gilead Sciences Research Scholar Award; a Pfizer ASPIRE Cardiovascular Award (all to J. S. C.); and the Howard Hughes Medical Institute (to A. M. G. and K. M. S.). The authors declare that they have no conflicts of interest with the contents of this article. The content is solely the responsibility of the authors and does not necessarily represent the official views of the National Institutes of Health.

This article contains Table S1 and Figs. S1–S4.

[1] To whom correspondence should be addressed: Division of Cardiology, Zuckerberg San Francisco General, Dept. of Medicine, University of California, San Francisco, 1001 Potrero Ave., Bldg. 100 Rm. 261, San Francisco, CA 94110. Tel.: 415-206-8315; Fax: 415-206-5447; E-mail: john.chorba@ucsf.edu.

[2] The abbreviations used are: PCSK9, proprotein convertase subtilisin/kexin type 9, LDL, low density lipoprotein; LDL-R, low density lipoprotein receptor; LDL-C, low density lipoprotein cholesterol; ER, endoplasmic reticulum; GOF, gain-of-function; LOF, loss-of-function; CHR, cysteine-histidine rich; Bis-Tris, 2-[bis(2-hydroxyethyl)amino]-2-(hydroxymethyl)propane-1,3-diol.

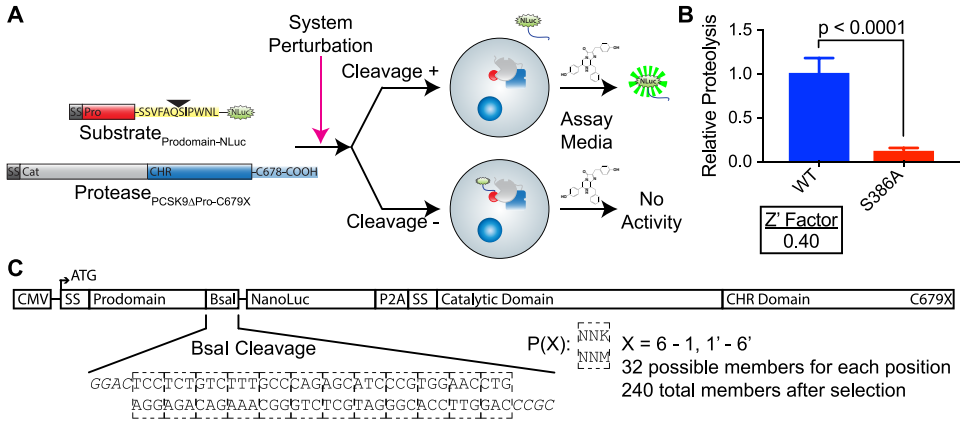

Figure 1. PCSK9 cleavage assay and mutagenesis library. *A*, schematic of the in *trans* PCSK9 proteolysis assay. Co-expression of the substrate (*Prodomain-NLuc*) with a non-secretable prodomain-deficient PCSK9 protease (*PCSK9ΔPro-C679X*) allows for secretion of the luciferase, and a positive readout in the conditioned medium, only when cleavage is permitted. In this situation, the system perturbation is a library of cleavage site mutants as substrates. See "Results" for further details. *B*, relative proteolysis of WT *versus* inactive (S386A) PCSK9 protease. *Error bars*, S.D. Results of an unpaired *t* test with Welch's correction and the *Z'* factor (62) are shown. *C*, schematic for design of a saturation mutagenesis library of proteolysis substrates. The design of the paired oligonucleotides to replace the BsaI cleavage site shown reflects the WT sequence, although each codon was sequentially exchanged for the NNK equivalent to generate the library. See "Results" for details.

mature protease. In addition, we modify our proteolytic assay to evaluate post-cleavage PCSK9 secretion and use our findings to identify residues differentially affecting proteolysis and secretion. We show that PCSK9 proteolysis is the rate-limiting step of PCSK9 secretion. Additionally, we apply our assays to clinically identified missense SNPs, finding that over half of these reported genetic alterations affect PCSK9 processing, suggesting a mechanism for many of these SNPs that are incompletely characterized. Through these SNPs, we also find regions of PCSK9 involved in allosteric modulation of its cleavage by loosening the substrate specificity of the active site from its native sequence. Overall, our findings suggest that PCSK9 proteolysis acts as a key structural switch whose regulation controls its ultimate function.

Results

A high-throughput luciferase-based assay for PCSK9 proteolysis

We first sought to develop a high-throughput method to assay PCSK9 proteolysis. In prior work, we showed that the PCSK9 catalytic domain can perform intermolecular proteolysis when co-expressing in *trans* a specific PCSK9 substrate (a proteolytically inactive PCSK9) along with an uninhibited PCSK9 protease (prodomain-deficient PCSK9) (16). Our prior system relied on immunoblot as the readout, which limited our throughput to analyze systemic perturbations. To improve this assay, we required a solution to the following biochemical challenges: 1) the intrinsically low output of a single-turnover protease, 2) the requirement of a cell-based environment to capture both protein folding and protease activity in the ER, and 3) the need for the protease to exist (and presumably fold) in complex with its inhibitory prodomain. Taking inspiration from PCSK9 itself, we hypothesized that by linking proteolytic cleavage to the secretion of an alternative but amplifiable reporter system, we could improve the absolute readout of a single-turnover event. Similarly, by designing the system to prevent secretion of the reporter in the absence of cleavage, we could attain an acceptable dynamic range. We thus constructed our protease substrate to contain the PCSK9 prodomain linked to a secretable luciferase (NanoLuc) (17), such that successful cleavage frees the luciferase to continue through the secretory pathway unlinked to PCSK9 and therefore unimpeded. As our goal was to assay PCSK9 proteolysis itself, we took advantage of the high affinity of the prodomain for the catalytic domain (12), as the two remain bound even in the presence of proteolysis- or secretion-abolishing mutations (16). Concomitantly, we engineered our prodomain-deficient PCSK9 protease to have a C679X truncation, so as to retain the entire PCSK9 complex within the ER, but have little to no effect on proteolytic function itself (Fig. 1*A*) (18, 19). We combined both engineered polypeptides on a single expression vector split by a viral P2A sequence to produce stoichiometric amounts of each (20, 21). Via transient transfections of this construct in 293T cells, and using the proportion of secreted luciferase as a proxy for cleavage, our assay provides a robust differentiation between proteolytically active (WT) and inactive (S386A) PCSK9 (Fig. 1*B*). Importantly, we assay both the luciferase activity in the conditioned medium as well as the luciferase activity of the cells themselves, as the latter measurement controls for well-to-well (and plasmid-to-plasmid) variations in transfection, transcription, and translation efficiency.

The substrate specificity of the PCSK9 protease is limited and explained by the structure of the mature protease

PCSK9 is known to cleave only itself, with its P6–P6′ cleavage sequence as SSVFAQ^{152} ↓ S^{153}IPWNL (22). Although the structure of mature PCSK9 is known, no structural data for proteolytically active proPCSK9 exist, leaving a need for thorough biochemical characterization. We were hopeful that the discovery of a complete substrate specificity profile might allow us to identify an improved substrate as the starting point for a competitive inhibitor or tell us more about the evolutionary trajectory of PCSK9. Previously, we had shown through an alanine scanning approach that residues at P4 (Val^{149}) and P3 (Phe^{150}) were particularly intolerant to change (16). Given the limited structure information provided through an alanine

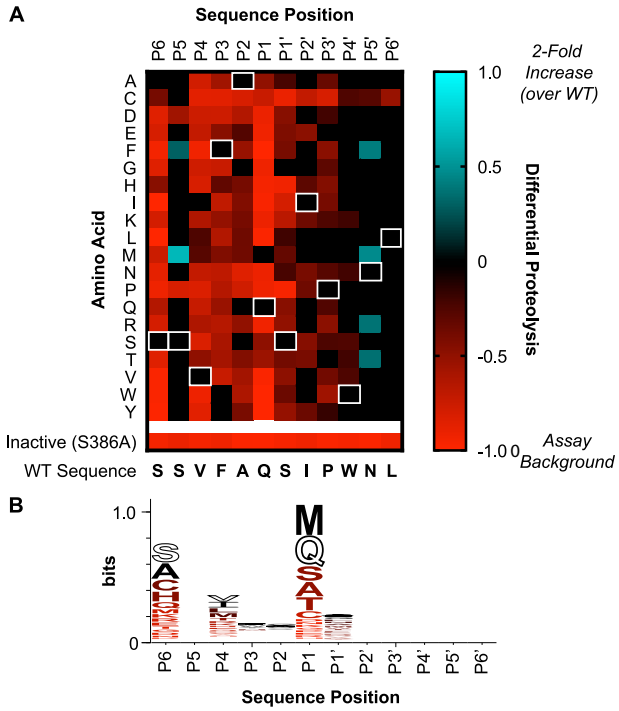

Figure 2. PCSK9 cleavage sequence specificity. *A*, heat map showing the relative cleavage for each single amino acid mutant in the P6–P6′ cleavage sequence as compared with the WT sequence. *White rectangles*, WT amino acid. A value of −1 (*red*) indicates essentially no proteolysis, and a value of +1 (*cyan*) indicates a 2-fold increase from the WT value. Mutants with statistically significant differences from WT, as determined by a Holm–Sidak corrected unpaired *t* test with $\alpha < 0.05$, are shown in *color*. Mutants with effects not statistically different are shown in *black*. *B*, WebLogo (27) illustrating the preferred cleavage sequence for PCSK9. The WT amino acid is shown *outlined* in *black*, with other residues *colored* to reflect the values in the heat map.

scan, we coupled our assay in hand with a saturation mutagenesis library at each of the P6–P6′ positions to more fully characterize potential PCSK9 substrates.

To create our library, we employed a Golden Gate cloning strategy using the Type IIS BsaI restriction enzyme (23, 24). We removed potential BsaI cleavage sites from our cleavage assay vector and installed a bidirectional BsaI cleavage site to allow the scarless insertion of paired oligonucleotides for the P6–P6′ positions (Ser^{147}–Leu^{158}) upon ligation. We sequentially used oligonucleotides containing the WT sequence with the exception of one NNK codon for each of the cleavage positions to generate the complete 240-member library (Fig. 1*C*). Each library member was confirmed by Sanger sequencing. We then assayed the effect of proteolysis for each positional mutant to find the relative amount of proteolysis for each mutant at a given amino acid position, with a value of 0 indicating no proteolysis and a value of 1 equivalent to the WT sequence (Fig. S1). The data are best visualized by showing the relative change in proteolytic activity compared with the WT residue only for those mutants with statistically significant differences (Fig. 2*A*).

In general, our results confirm and expand upon previous mutational analysis of PCSK9 intramolecular cleavage(22, 25, 26) and correlate well with the crystal structure of mature PCSK9 (12, 14, 15). Positions P6, P4, and P1 showed a very narrow sequence specificity, allowing only similar substitutions to the WT sequence and with most substitutions showing markedly reduced cleavage efficiency. Positions P3, P2, and P1′ also showed a narrow sequence specificity, although overall, substitutions here appeared mildly less detrimental than those at P6, P4, and P1. These differences are reflected in the sequence logo (27) (Fig. 2*B*), which highlights the preferred residues. In the known crystal structure of PCSK9, the P6 serine and the P4 valine side chains protrude directly into a narrow hydrophobic binding pocket, explaining why only the P6 Ser → Ala and the P4 Val → Ile mutations are fully tolerated (Fig. 3). The P3 phenylalanine points away from the binding pocket but forms a π-π stacking interaction with Trp^{72} of the prodomain, which itself probably interacts with Phe^{318} of the catalytic domain. The importance of this π-π stacking explains the tolerance at P3 for the other aromatic residues, Trp and Tyr. Additional steric bulk is tolerated, albeit poorly, at the P2 position. For the P1 position, the hydrogen bond made by the lone pairs from the amide carbonyl of the glutamine side chain with the free amide of Asn^{317} of the catalytic domain appears to be very important, as only a methionine residue, which could similarly position its thioether lone pairs, is well-tolerated. The presence of a ridge, rather than a binding groove, for C-terminal cleavage positions explains the need for flexibility at P1′ and the tolerance for small residues like glycine, serine, and alanine. The flexibility at P5, particularly for larger positions, correlates well with the lack of strict conservation at this residue (Phe in *Mus musculus*, Leu in *Rattus norvegicus*) as well as the protrusion of the side chain away from the binding groove and into a solvent-exposed space. The identities of P2′–P6′ have little effect on cleavage, consistent with the lack of a potential binding pocket for these residues.

The majority of mutations investigated caused a loss of proteolysis, an expected result, taking an unbiased mutagenesis approach to an area of the protein critical for its ultimate function. Several mutations at P5 and P5′ showed mild improvement compared with the WT sequence. To rule out the possibility of an alternative transcriptional start site biasing NanoLuc production, we compared the P5 M, P5′ M, and WT cleavage sequences with the inactive S386A protease, confirming no difference in readout (Fig. S2*A*). We then investigated the possibility of synergistic mutations at these sites, pairing each of the mutations at P5 and P5′ sites that showed improved cleavage readouts. Our results showed no evidence of synergy between the double mutations (Fig. S2*B*), with all but one double mutant not significantly different from WT in cleavage activity.

Overall, our results suggest that the PCSK9 cleavage sequence is essentially optimized with its native sequence, with areas of tolerance unlikely to provide significant improvement on proteolytic activity. In addition, the structure of the mature protein helps to explain the sequence specificity for PCSK9 cleavage, which is fairly well-conserved among interspecies PCSK9 genes (28). Our results support the argument that the need to preserve a cleavable sequence as part of a conformational switch has driven the evolution of the P6 and P4–P1′ amino acids. By contrast, a different mechanism probably drives the evolutionary conservation of the P2′–P6′ amino acids. Indeed, after cleavage, these residues form an α-helix over 20 Å away from the active site, with recent data suggesting that the structure of this helix, in particular residues Trp^{156}–Ile^{161}, covers a binding site on

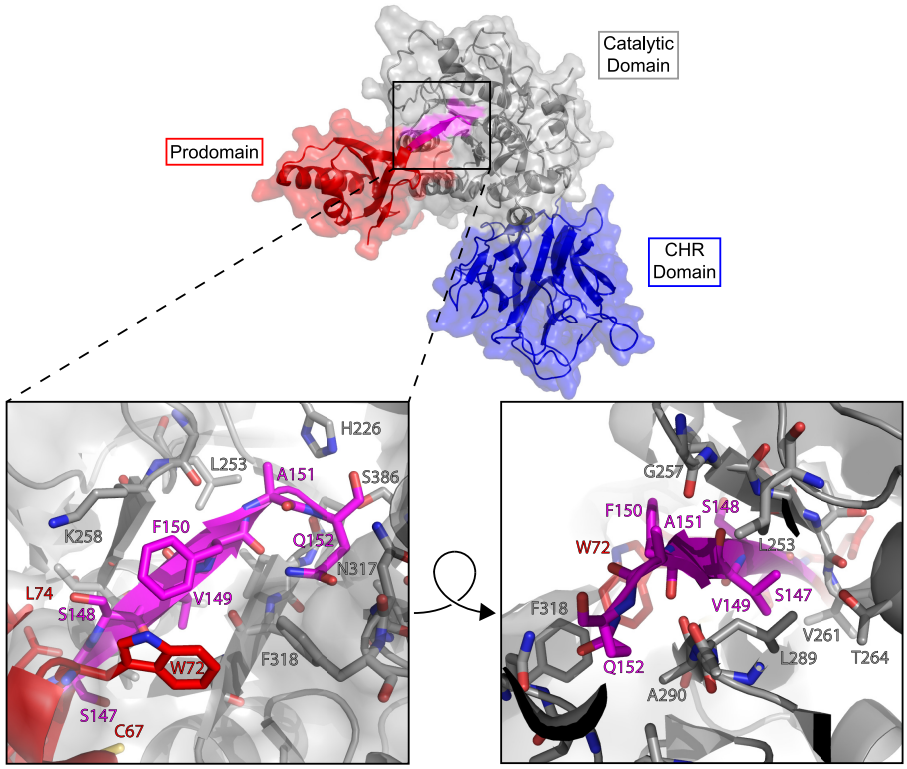

Figure 3. Crystal structure of the PCSK9 active site and bound prodomain tail. Shown is the structure of mature PCSK9 (Protein Data Bank code 2P4E) (12) with missing internal loops optimized by ModLoop (63). The active site with the bound prodomain C terminus (*magenta*, residues 147–152) is *magnified*, and the residues are identified. The *right panel* shows a *cut-away view* of the prodomain residues protruding directly into the binding groove. See "Results" for discussion.

the catalytic domain important in stabilizing the interaction with the EGF(A) domain of the LDL-R (29).

A stepwise analysis of PCSK9 processing illustrates residues differentially regulating proteolysis and secretion

Previously, we reported that the identity of residue 152 (the P1 residue) could differentially regulate proteolysis and secretion (16). We thus asked whether additional residues within the prodomain tail and bound to the active site (residues P6–P1) could act similarly. We designed an alternative assay scheme to evaluate post-cleavage PCSK9 secretion based on a prior in *trans* secretion system (Fig. 4*A*) (30). Here, we altered our bicistronic co-expression system to include an unmodified PCSK9 prodomain as well as a prodomain-deficient PCSK9 with a C-terminally tagged luciferase. Again using transient transfections in 293T cells and evaluating the conditioned medium and the transfected cells separately for luciferase activity, we found that our assay reliably differentiated secretory (WT) PCSK9 from secretion-restricted (S462P) (31) PCSK9 (Fig. 4*B*).

Focusing on the post-cleavage residues bound in the active site, we then created a similar single amino acid saturation mutagenesis library for the P6–P1 positions and evaluated the effects of each library member against in *trans* PCSK9 secretion (Fig. 4*C*). Similar to the proteolysis assay, positions P6 and P4 were severely intolerant to mutation, whereas the P5 position was mostly accommodating of mutational change (Fig. 5 (*A* and *B*) and Fig. S3). A direct comparison between proteolysis and secretion phenotypes revealed several interesting results (Fig. 5*C*). Despite the relative intolerance of the P4 position to mutation in either assay, charged residues, particularly basic ones, were less detrimental in the proteolysis assay as compared with the secretion assay, where they essentially abolished secretion. This suggests that the transition state for the proteolytic cleavage step is more tolerant of an ionic charge at this position than is the cleaved, mature PCSK9 awaiting secretion. Conversely, several of the mutations in P1, particularly those installing branched aliphatic chains, were less detrimental in the secretion assay than in the protease assay, where essentially no proteolysis was seen. The biochemistry of the protease probably explains this phenomenon; the side chain of Asn^{317} stabilizes the oxyanion hole filled by the proteolytic transition state, in turn facilitated by hydrogen bonding with Gln^{152} (or Q152M). After proteolysis, however, only the space occupied by the glutamine side chain remains important, while the requirement to accept hydrogen bonds does not. Overall, these data correlate well with our previous findings (16).

PCSK9 proteolysis is the rate-limiting step of PCSK9 secretion

Among the residues evaluated in both assays, only one mutant, P6-C (S147C), revealed a phenotype of improved secretion and reduced proteolysis when each was compared with WT. We recognized this unique profile as a means to biochemically test whether PCSK9 proteolysis is the rate-limiting step of PCSK9 secretion, a concept that is consistent with previous literature but has not been tested directly (22, 25, 26). To confirm that our evaluation of intermolecular PCSK9 proteolysis correlates with autoproteolysis of full-length PCSK9, we installed the S147C mutation into a full-length PCSK9 harboring a C-terminal BirA*-FLAG tag. Immunoblots of lysates of 293T cells overexpressing both WT and S147C tagged PCSK9

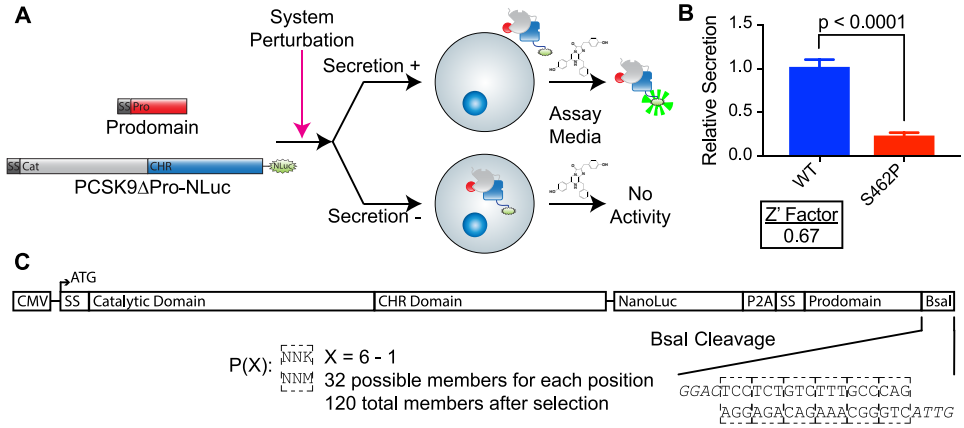

Figure 4. PCSK9 secretion assay and mutagenesis library. *A*, schematic of the in *trans* PCSK9 secretion assay. Co-expression of the prodomain with a luciferase-tagged, prodomain-deficient PCSK9 (*PCSK9ΔPro-NLuc*) allows for readout of the luciferase in the conditioned medium only when secretion of the PCSK9 is permitted. In this situation, the system perturbation is a library of prodomain tail mutants. See "Results" for details. *B*, relative proteolysis of WT *versus* non-secreted (S462P) PCSK9 protease. *Error bars*, S.D. Results of an unpaired *t* test with Welch's correction and the *Z'* factor (62) are shown. *C*, schematic for design of saturation mutagenesis library of secretory prodomain tail mutants. The design of the paired oligonucleotides to replace the BsaI cleavage site shown reflects the WT sequence, although each codon was sequentially exchanged for the NNK equivalent to generate the library. See "Results" for details.

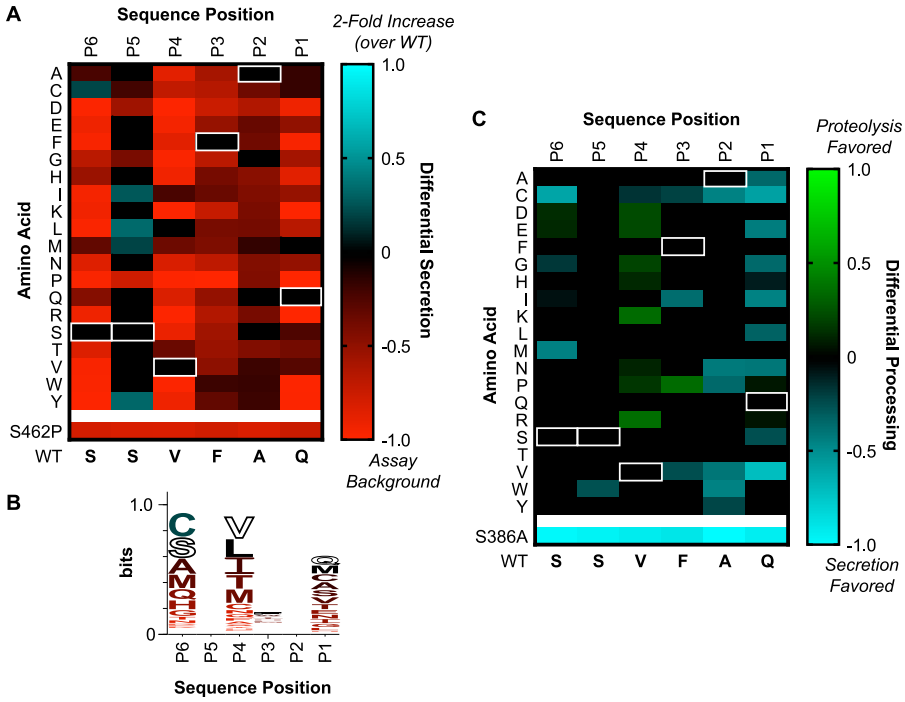

Figure 5. PCSK9 secretion sequence specificity. *A*, heat map showing the relative secretion for each single amino acid mutant in the P6–P1 cleavage sequence as compared with the WT sequence. *White rectangles*, WT amino acid. A value of −1 (*red*) indicates essentially no secretion, and a value of +1 (*cyan*) indicates a 2-fold increase from the WT value. Mutants with statistically significant differences from WT, as determined by Holm–Sidak corrected unpaired *t* test with $\alpha < 0.05$, are shown in *color*. Mutants with effects not statistically different are shown in *black*. *B*, WebLogo (27) illustrating the preferred secretion sequence for PCSK9. The WT amino acid is shown *outlined* in *black*, with other residues *colored* to reflect the values in the heat map. *C*, heat map showing the differential cleavage for the single-amino acid mutants in the proteolysis *versus* secretion assays. Mutants with statistically significant differences between proteolysis and secretion assays, as determined by Holm–Sidak corrected unpaired *t* test with $\alpha < 0.05$, are shown in *color*. Mutants with effects not statistically different are shown in *black*. Values in *green* illustrate preferential proteolysis, whereas those in *cyan* illustrate preferential secretion.

show that the ratio of mature to total PCSK9 is higher for the WT construct as compared with the mutant (Fig. 6*A*). These findings are consistent with intramolecular proteolysis being delayed similarly to the intermolecular proteolysis evaluated in our high-throughput assay. We then installed the S147C mutation into the C-terminally NanoLuc-tagged full-length PCSK9 construct and performed a similar luciferase-based secretion assay. We found that overall secretion of the full-length S147C was less than that of the WT construct (Fig. 6*B*). Given that the S147C PCSK9 has a proteolysis defect but a mild secretion advantage, we conclude that proteolysis is the rate-limiting step of WT PCSK9 secretion.

Missense SNPs in PCSK9 frequently affect proteolytic function

Given the importance of proteolysis in PCSK9 maturation, we then utilized our proteolysis assay to survey the landscape of missense SNPs reported in the clinical literature. We selected 84 total mutants from non-redundant SNPs from two well-

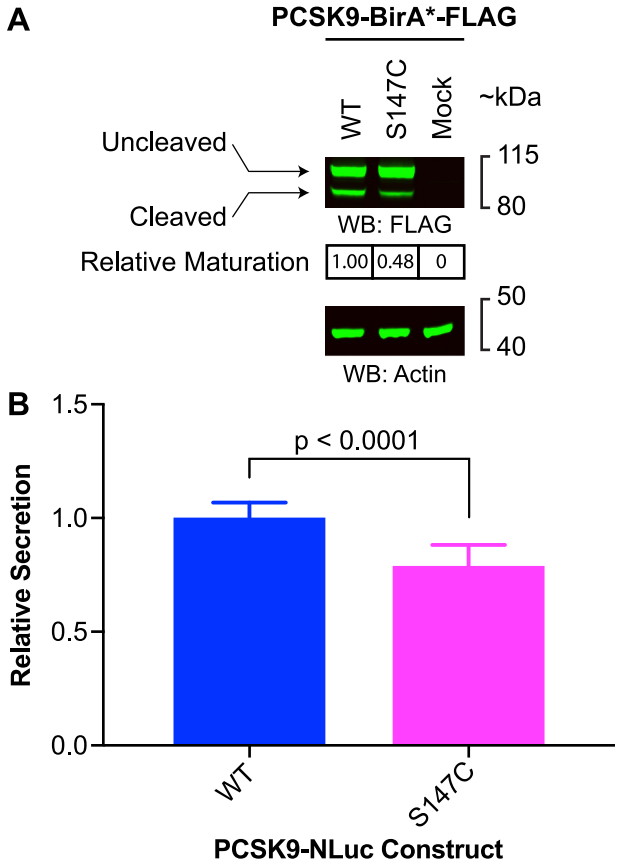

Figure 6. Cleavage is the rate-limiting step of PCSK9 processing. *A*, immunoblot of cell lysates transiently expressing PCSK9-BirA*-FLAG WT or S147C constructs. The relative maturation, as quantified on the immunoblot, is noted *below* the appropriate *column*. *B*, relative secretion of full-length PCSK9 WT *versus* S147C, as measured by luciferase activity. *Error bars*, S.D. Results of an unpaired *t* test with Welch's correction are shown.

curated databases as well as certain site mutants made for selected biochemical studies (13, 32–34). We then installed each of these mutations through site-directed mutagenesis into our proteolysis assay vector, confirming their identities through extensive sequencing, and ran the proteolysis assay alongside our positive (WT) and negative (S386A inactive) controls. Overall, we found that 47 of the 84 mutants surveyed (56%) caused a statistically significant change in proteolysis, about equally distributed between improved and reduced proteolytic function, although the absolute changes were quite modest (Fig. 7 and Table S1). Our assay recapitulated the findings of many of the known SNPs previously characterized to cause reduction in self-proteolysis, including loss-of-function (LOF) mutations G106R (35), Q152H (25), and N354I (36) as well as gain-of-function (GOF) mutations S127R (22, 37) and D129G (38). SNPs reported in the prodomain tended to cause a loss of proteolytic activity, whereas SNPs in the catalytic and cysteine-histidine rich (CHR) domains tended to cause improvements in proteolytic activity.

Missense SNPs in PCSK9 can affect proteolysis-independent secretion

To fully characterize the effects of these SNPs on PCSK9 processing, we analyzed all but one of these SNPs using our PCSK9 secretion assay. Here, we found a smaller number of mutants (26 of 84) to affect in *trans* secretion, with all but two having a detrimental impact (Fig. 7). As in the protease assay, we confirmed the findings of mutations previously shown to reduce PCSK9 secretion by sequestration in the ER, including G236S (36) and S462P (31). Most of the affected SNPs resided in the prodomain, consistent with the purported role of the prodomain as a chaperone to assist with overall protein folding. Only L108R and A168E showed modestly improved secretion. As these results were similar to the findings in the proteolysis assay, we suspect that these mutations may improve the rate of protein folding overall.

Combining the results of our assays, we characterized the SNPs into three categories based on their effect on processing: improved, reduced, and unchanged (Table 1). 34 SNPs (40%) showed improved processing, exclusively due to improved proteolytic ability, where 23 SNPs (27%) showed decreased processing, split nearly equally between decreased proteolysis or decreased protease-independent secretion. Thus, two-thirds of the SNPs showed a phenotype affecting some aspect of processing. In addition, among SNPs of uncertain clinical significance, defined as those with either no known associated phenotype or a possible but unconfirmed phenotype (53 total), 30 SNPs could potentially be functionally reclassified (Table 1, *boldface type*). Last, 11 SNPs displayed processing phenotypes discordant with what would be expected according to their proven or suggested effects on LDL-C (Table 1, *italic type*). For many of these particular SNPs, the processing effects were quite modest. However, this also illustrates that additional mechanisms, beyond PCSK9 processing alone, can and do play more significant roles in driving serum LDL-C levels.

Mutations in PCSK9 distal to the active site can allosterically modulate proteolytic function

We were struck by the spatial clustering of certain SNPs in affecting proteolytic function, particularly when mapped onto the crystal structure of mature PCSK9. In particular, in the minimal L-loop of the PCSK9 prodomain (Ser^{127} and Asp^{129}), mutations reduced proteolysis, whereas along the unstructured loop on the catalytic domain containing a furin cleavage sequence (Arg^{215}, Phe^{216}, Arg^{218}, Gln^{219}) (18), mutations improved cleavage. Additionally, mutations spread through the CHR domain tended to correlate with improved proteolytic ability, consistent with previous evidence that the CHR domain may interact with the prodomain (39). To investigate the possibility that certain regions could allosterically modulate PCSK9 proteolysis, we selected several SNPs with improved proteolytic ability and evaluated their effects on the sequence specificity of the protease (Fig. 8*A*). In comparing relative proteolysis with that of the WT cleavage sequence, R215H showed a profile of increased tolerance for the P1A (Q152A) and P1′Q (S153Q) cleavage sequences (Fig. 8*B*). By contrast, A245T appeared markedly similar to the WT protease, and L108R, although showing no significant difference from WT, qualitatively appeared to have an intermediate phenotype (Fig. 8*B*). These data suggest that the R215H protease allows more flexibility in the cleavage sequence, both in permitting a loss of hydrogen bonding between Gln^{152} and Asn^{317} and in allowing increased size at the P1′ position. Whereas L108R and A245T

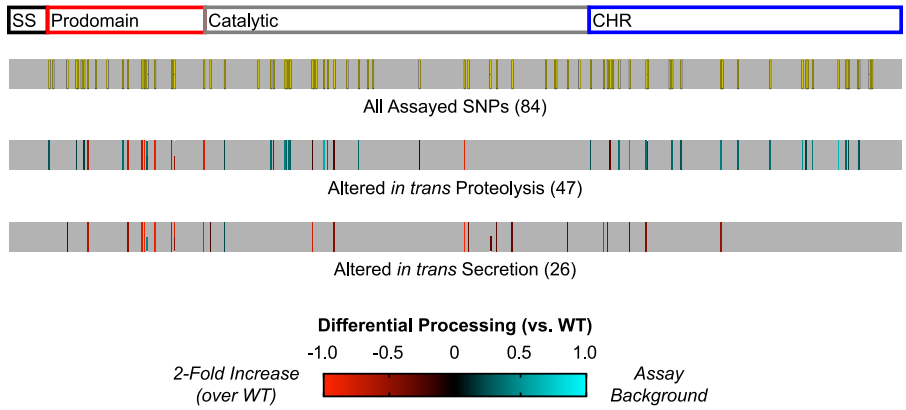

Figure 7. Clinical SNPs frequently affect PCSK9 processing. *Top,* individual SNPs chosen for analysis graphically represented as *yellow bars* with *black outlines* on the protein primary structure, with PCSK9 domains noted *above*. Residues with two SNPs at a given position are denoted by two *half-height bars stacked vertically*. *Middle*, SNPs with statistically significant differences in proteolysis compared with WT, as determined by Holm–Sidak corrected unpaired *t* test with $\alpha < 0.05$. A value of -1 (*red*) indicates essentially no processing activity, and a value of $+1$ (*cyan*) indicates a 2-fold improvement over WT. *Bottom*, SNPs with statistically significant differences in secretion compared with WT, as determined by a Holm–Sidak corrected unpaired *t* test with $\alpha < 0.05$. The *color scheme* is the same as for the proteolysis assay.

permit increased proteolysis overall, this does not translate into a selective advantage for a particular sequence profile. These differential findings imply structure–activity relationships suggestive of specific allosteric effects.

The unstructured furin cleavage sequence in the catalytic domain is located in close proximity to the active site and, like the native 147–153 SSVFAQS cleavage sequence, is immediately preceded by an EED motif. We thus hypothesized that this sequence could act as a competitive inhibitor of the native cleavage sequence in the uncleaved proPCSK9. We directly substituted residues 212–220 of full-length PCSK9 (encoding GTRFHRQA) for the SSVFAQS cleavage sequence in an attempt to optimize that region for active site binding. However, secretion of full-length PCSK9 was mildly improved with this substitution (Fig. 8*C*), inconsistent with this region acting as a competitive inhibitor although consistent with the region tolerating significant mutation. Moreover, when the same substitution was placed in Q152V PCSK9 (which eliminates proteolysis at residue 152), no secretion was observed. This indicates that the engineered alternative sequence cannot undergo proteolysis and rescue the secretion phenotype when the native cleavage sequence also cannot be cleaved. Along similar lines, neither direct substitution nor an insertion of the SSVFAQS optimized cleavage sequence at residues 212–220 produced substantial differences in either of our dedicated in *trans* proteolysis or secretion assays (Fig. S4). When taken together with the differential effects of the R215H mutation on the cleavage sequence, these data argue that the unstructured furin cleavage loop acts as a negative allosteric modulator of PCSK9 cleavage.

Discussion

In this work, we developed a cell-based, high-throughput method to evaluate the sequence specificity of a single-turnover protease, previously only known to cleave itself at the SSVFAQ↓SIPWNL sequence. We provide biochemical evidence that the sequence specificity is quite restricted at the P6 and P4–P1′ residues and that only modest improvements to the native cleavage sequence are possible through single-amino acid mutagenesis. Although the limitations of generalizing the results of our assay to WT PCSK9 include our design of intermolecular (rather than intramolecular) proteolysis as well as the need for an overexpression system, our results correlate well with the structure of the mature, cleaved PCSK9. No structure of the uncleaved proPCSK9 has been reported.

The advantages of our assay system include its ease of use, scalability, and enzymatically amplified readout. We anticipate that our assay system would be generalizable to other low-activity proteases. In theory, the system could be applied to any protease capable of proper folding in the secretory pathway, so long as the target cleavage sequence could be linked to an intracellular anchor and successful cleavage could free the luciferase for secretion. Indeed, similar secretable luciferase-based assays have been used as biosensors for caspase activation and viral cleavage (40–42). Here, we used the native PCSK9 prodomain as our cleavage target. However, in a system not reliant upon the presence of an autoinhibitor, the cleavage sequence could be sequestered to particular compartments by choosing an appropriate type I membrane protein as the anchor. In so doing, one could probe protease activity in specific compartments. Similar approaches using a release of luciferase from pro-IL-1-β protein aggregates have been used to probe protease activity in the inflammasome (43).

We applied our system to evaluate clinical SNPs found in PCSK9, a key modulator of serum LDL-C and an attractive cardiovascular target. Our findings suggest that alteration in PCSK9 proteolytic function is a frequent effect of SNPs that present in a clinical setting. For some mutants, alterations in PCSK9 processing alone may be enough to cause the phenotype observed. The E32K and R93C mutants serve as examples at each extreme: the increased cleavage of the E32K mutant probably drives higher serum PCSK9, which in turn lowers LDL-C, whereas the reduced cleavage of R93C causes the opposite effect. In a general Japanese population, the E32K mutation correlates with lower serum PCSK9 levels, consistent with our proposed mechanism (44). However, the correlation between serum PCSK9 and genotype in other populations is variable (45), with efforts to measure serum PCSK9 as a means to iden-

Table 1
Effect of SNPs on PCSK9 processing

Boldface type, potential reclassification. *Italic type*, indicates discordance with described LDL-C phenotype. LDL-C phenotypes are illustrated by *colors* (*cyan*, GOF/high LDL-C; *magenta* LOF/low LDL-C), with color intensity reflective of confidence of assignment (*bright*, confident; *light*, proposed but unconfirmed).

PCSK9 Processing				
Increased		Decreased		Unchanged
Proteolysis	Secretion	Proteolysis	Secretion	
E32K		*A62D*	R46L	D35Y
A53V		R93C	*D129N*	E54A
G59R		R104C	**N157K**	E57K
S89L		G106R	G236S	A68T
L108F		V114A	***R357H***	T77I
L108R		*S127R*	*D374Y*	R194Q
A168E		*D129G*	F379A	R237W
D204N		Q152H	**H391N**	A239D
E206K		L253F	R434W	G263S
R215H		**R319W**	S462P	P279T
F216L		N354I	***S465L***	L283M
R218S		*P467A*		D374H
Q219E				H417Q
A245T				I424V
R248H				N425S
R272Q				A443T
G452D				R469W
V474I				N513D
E482G				A514T
R495Q				Q554E
R496Q				E620K
R496W				D651Y
F515L				R659L
A522T				S668G
H553R				S668R
W566S				E669K
H591Q				G670E
P616L				
Q619P				
V624M				
V644I				
V650I				
N652D				
D660N				

tify carriers of certain PCSK9 mutations seeing mixed success (46, 47). Serum PCSK9 levels undergo significant fluctuations, compared with the more stable LDL-C (48–50), probably contributing to this difficulty. As a result, our assay may provide additional value in evaluating the likely effect of a novel clinically identified SNP and can be readily performed in any standard biological laboratory with the capacity for PCR, mammalian tissue culture, and a plate reader. As others have noted, relatively modest changes in LDL-C caused by PCSK9 mutations produce lifelong effects, leading to an effectively lower "cumulative dose" of LDL-C on the vasculature over many years (6). Thus, small biochemical effects on PCSK9 processing may very well be clinically relevant.

Although our ability to categorize the SNPs based on processing ability is helpful, it also illustrates the complexity of PCSK9 physiology. For some mutations, the effects on processing are likely to be overshadowed by their other effects, such as LDL-R binding (D374Y) (34, 51) or cleavage and degradation by other proteases (F216L) (18, 52). For other mutations, these additional effects can explain the discordance between processing phenotype and functional classification. For SNPs with increased proteolytic function but LOF (low LDL-C) phenotypes, for example, A522T has previously been shown to have an overall secretion-restricted phenotype (53), consistent with the presence of additional requirements for secretion post-cleavage, whereas the Q219E mutation has been shown to render the protein more susceptible to furin-mediated cleavage (18). Similarly, some mutants with reduced cleavage show GOF (high LDL-C) phenotypes, and the S127R mutation is a prime example. Prior well-conducted pulse-chase studies have shown the rate of PCSK9 maturation in the S127R mutant to be slower than that of WT (37); however, these studies looked at total PCSK9 from cellular lysates and therefore could not definitively exclude an increased rate of intracellular degradation of S127R PCSK9, compared with WT, as an explanation. Our assay, looking at proteolysis alone, provides compelling evidence to support the fact that PCSK9 proteolysis is hindered by this mutation. The mechanism by which S127R PCSK9 causes a GOF phenotype, however, despite its impaired processing and secretion, remains to be defined.

Whereas PCSK9 has several transcriptional regulators, it is strongly induced by SREBP-2 (54), the same sterol sensor up-regulated by 3-hydroxy-3-methylglutaryl-CoA reductase inhibitors to increase LDL-R transcription. This has led to the recognition that statin therapy induces PCSK9 production (55), which blunts some of the cholesterol-lowering effect. Mutants in PCSK9 that enhance processing would probably have an amplified response to statin therapy and therefore exhibit lower-than-expected responses. Whether such genotypes could predict response to statins deserves further study. Additionally, such genotypes may also predict a higher likelihood to receive benefit from anti-PCSK9 therapies currently in clinic.

Our work also illustrates the power of clinical findings in illustrating the native biology of our protein of interest. Although by no means an unbiased sample, the clinical SNPs evaluated revealed that a sizeable proportion of them affected proteolytic function, and we provide evidence that some mutations allosterically regulate this function. This is not altogether surprising; allosteric regulation of enzyme substrate specificity has been described in many enzyme classes. Kinases in the DYRK family regulate their specificity by first performing self-phosphorylation of tyrosine residues, allowing a conformation change that permits ultimate serine/threonine phosphorylation of targets (56). Metabolic enzymes, such as lipoxygenases and transcarbamylases, alter their specificity through allosteric regulation by their products (57, 58). Small molecules have been used to allosterically regulate the specificity for broad proteases, such as γ-secretases, away from pathogenic substrates, such as amyloid precursor protein (59). Given that targeting

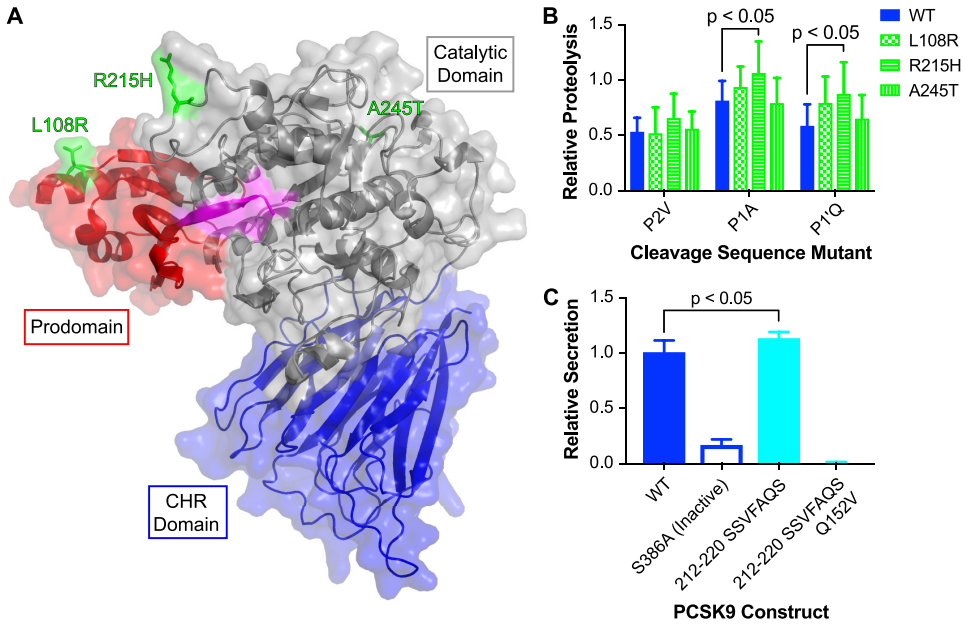

Figure 8. Allosteric effects of PCSK9 SNPs. *A*, crystal structure of mature PCSK9 (Protein Data Bank code 2P4E) (12) with missing internal loops optimized by ModLoop (63), with selected SNPs with improved proteolytic ability *labeled* in *green*. *B*, effect of individual SNPs on proteolytic activity of selected cleavage sequence mutants. To compare the effect of the SNPs on sequence specificity, values are normalized to the activity of that SNP on the WT cleavage sequence. *Error bars*, S.D. Results of unpaired *t* tests with Welch's correction are shown. *C*, effect of optimized cleavage sequence (SSVFAQS) replacing the native 212–220 (GTRFHRQA) sequence in full-length PCSK9-NanoLuc on relative secretion. *Error bars*, S.D. Results of an unpaired *t* test with Welch's correction are shown.

PCSK9 remains of great interest to the cardiovascular community, this latter example is particularly relevant. A strategy that may phenocopy and induce the allosteric effects of these SNPs, whether by a small molecule or by other means, may be a reasonable approach to ultimately reduce PCSK9 function and lower LDL-C in the clinic.

Experimental procedures

Materials and reagents

Oligonucleotide primers were custom synthesized by Elim Biopharmaceuticals (Hayward, CA). Restriction enzymes and polymerases were purchased from New England Biolabs (Ipswich, MA). Mouse monoclonal antibody to FLAG (clone M2) was obtained from MilliporeSigma (St. Louis, MO). Mouse monoclonal antibody to β-actin (8H10D10) was obtained from Cell Signaling (Danvers, MA). Goat anti-mouse IRDye 800CW conjugate secondary antibody was obtained from LI-COR Biosciences (Lincoln, NE). Coelenterazine was obtained from Gold Biotechnology (St. Louis, MO). All other reagents were obtained from MilliporeSigma unless otherwise noted.

Plasmid construction

All expression vectors were created by Gibson assembly (60) after PCR amplification of appropriate PCSK9 domains from plasmids described previously (16), a plasmid encoding nanoluciferase (Promega, Madison, WI), or a plasmid encoding the BirA*-FLAG tag (generous gift from R. Huttenhain and N. Krogan, University of California, San Francisco) into the pcDNA5/FRT/TO backbone (Thermo Fisher Scientific, Waltham, MA). Viral P2A sequences and linkers were added during Gibson assembly via appropriate oligonucleotide design. For saturation mutagenesis library vectors, the removal of BsaI restriction sites and creation of a bidirectional BsaI cleavage site at the cleavage site (cleavage library) or prodomain C terminus (secretion library) was performed by site-directed mutagenesis using partially overlapping primers, as described previously (61). Individual point mutations for SNPs and for SNP-based cleavage site mutations were also installed using site-directed mutagenesis. All constructs were extensively sequenced to ensure the absence of errors.

Saturation mutagenesis library generation

A series of paired, complementary oligonucleotides were designed containing 4 nucleotides of overhang to the library vector, followed by either 36 (cleavage library, P6–P6′) or 18 (secretion library, P6–P1) nucleotides of the WT sequence. For each pair, one of the codons was designed as NNK (forward) or MNN (reverse), for 12 (cleavage library) or 6 (secretion library) pairs total. 10 μM solutions of oligonucleotide pairs were then phosphorylated by T4 PNK (New England Biolabs) at 37 °C for 30 min, followed by denaturation at 95 °C for 5 min and then a 0.1 °C/s ramp to 25 °C to anneal. 50 ng of library vector was then subjected to simultaneous digestion by BsaI-HF (New England Biolabs) and ligation by T7 DNA ligase (New England Biolabs) in the presence of 4 nM phosphorylated oligonucleotide pair, cycling between 37 and 23 °C for 5 min each for six total cycles. The ligation reaction was treated with PlasmidSafe exonuclease (Epicenter, Madison, WI) at 37 °C for 30 min, followed by transformation into chemically competent Mach1 cells (Thermo Fisher Scientific). After sufficient growth at 37 °C, colonies were screened by colony PCR using oligonucleotide primers flanking the insertion sequence. PCR products were purified using a ZR-96 DNA Clean & Concentrator kit (Zymo Research, Irvine, CA) and subjected to Sanger sequencing. Desired clones not identified on initial sequencing were created by designing

oligonucleotide pairs containing the desired sequence and performing cloning as noted above.

Cell culture

HEK293T cells were obtained from ATCC (Manassas, VA) and maintained in high-glucose, L-glutamine and pyruvate supplement DMEM (Thermo Fisher Scientific) supplemented with 10% fetal bovine serum (Axenia BioLogix, Dixon, CA) at 37 °C in 5% CO_2.

High-throughput luciferase assays

HEK293T cells were seeded into white-bottomed 96-well plates at 2×10^4 cells/well on the day before transfection. On the day of transfection, medium was changed, and cells were transfected with Lipofectamine 3000 (Thermo Fisher Scientific) according to the manufacturer's protocol using 40 ng of DNA/well. Cells were incubated at 37 °C for 24 h. At the time of readout, one-half of the conditioned medium was transferred to a fresh white-bottomed 96-well plate. Luciferase activity was measured in the conditioned medium by adding a 1:1 mixture of filtered 2× coelenterazine non-lytic reagent (300 mM sodium ascorbate, 5 mM NaCl, 0.1% BSA, 40 μM coelenterazine) and incubating at room temperature on a shaker in the absence of light for 5–10 min, followed by immediate readout of luminescence on a plate reader (Tecan Systems, San Jose, CA). Luciferase activity was measured in the cells simultaneously using a filtered 2× coelenterazine lytic reagent, with 0.1% Triton X-100 instead of BSA. All assays were performed in triplicate and repeated at least three times.

Data analysis

Data analysis was performed using Prism version 7.0 (GraphPad Software, La Jolla, CA). The proportion of secreted over total (secreted plus cellular) luciferase activity was calculated for each well. Data were normalized to WT and negative control samples included on each plate. Data were cleaned to remove wells with poor transfection efficiency (identified by poor cellular luminescence readout) and then for potential outliers (using the ROUT method, with a maximum false discovery rate of 1%). For library analyses, data were compiled into tables by grouping results from each amino acid position and normalized within that group. Statistical significance for each mutation was evaluated using multiple unpaired *t* tests corrected for multiple comparisons using the Holm–Sidak method and α of 0.05. Heat maps were then generated showing the normalized activity scores (where 0 indicated no activity, and 1 indicated WT level activity) and the S.D. values of those scores. Additional heat maps were generated by using the difference in normalized activity of each amino acid mutant compared with the WT sequence and plotting only those values that were statistically significant. Sequence logos were created by the WebLogo3 web application (27) via position-weight matrix files generated from the normalized activity scores. Data analysis for the SNP assays was essentially similar.

Western blot analyses

HEK293T cells were seeded in 6-well plates at 5×10^5 cells/well on the day before transfection. On the day of transfection, medium was changed, and cells were transfected with Lipofectamine 3000 (Thermo Fisher Scientific) according to the manufacturer's protocol using 1 μg of DNA/well. Cells were incubated at 37 °C for 24 h. Cells were then washed with ice-cold PBS twice, resuspended in ice-cold PBS, transferred to a microcentrifuge tube, and centrifuged at 300 × *g* for 5 min. PBS was aspirated, and cell pellets were resuspended on ice in 40 μl of lysis buffer (50 mM Tris-HCl, pH 7.4, 150 mM NaCl, 0.1% Nonidet P-40, 1× cOmplete protease inhibitor mixture). Lysates were clarified at 21,000 × *g* for 15 min, and protein concentration was quantified by BCA assay. Gel samples were made in SDS-based Laemmli buffer under reducing conditions, heated at 98 °C for 5 min, and loaded onto 4–12% BisTris SDS NuPAGE precast gels (Thermo Fisher Scientific) for electrophoresis. The size-separated proteins were then transferred to nitrocellulose. The blots were blocked in 5% nonfat dry milk in Tris-buffered saline (20 mM Tris, pH 7.4, 150 mM NaCl) containing 0.1% Tween (TBS-T) for 1 h. The appropriate primary antibodies were hybridized to the blots overnight at 4 °C. The blots were washed three times for 10 min each with TBS-T, and the appropriate secondary antibodies were hybridized in 5% nonfat dry milk in TBS-T for 1 h at room temperature. The blots were again washed three times for 10 min each with TBS-T before directly imaging with the ODYSSEY infrared imaging system (LI-COR Biotechnology). Quantification was performed with the LI-COR imaging software.

Author contributions—J.S.C. conceptualization; J.S.C. and A.M.G. data curation; J.S.C. and A.M.G. formal analysis; J.S.C. and K.M.S. supervision; J.S.C. and K.M.S. funding acquisition; J.S.C. and A.M.G. investigation; J.S.C. methodology; J.S.C. writing-original draft; J.S.C., A.M.G., and K.M.S. writing-review and editing; K.M.S. project administration.

Acknowledgments—We thank Prof. Charles Craik (University of California, San Francisco) and members of the Shokat laboratory for helpful discussions. We also thank Dr. Patricia Dranchak and Prof. James Inglese (NCATS, National Institutes of Health) for helpful assistance with the design of high-throughput assays.

References

1. Park, S. W., Moon, Y. A., and Horton, J. D. (2004) Post-transcriptional regulation of low density lipoprotein receptor protein by proprotein convertase subtilisin/kexin type 9a in mouse liver. *J. Biol. Chem.* **279,** 50630–50638 CrossRef Medline
2. Maxwell, K. N., Fisher, E. A., and Breslow, J. L. (2005) Overexpression of PCSK9 accelerates the degradation of the LDLR in a post-endoplasmic reticulum compartment. *Proc. Natl. Acad. Sci. U.S.A.* **102,** 2069–2074 CrossRef Medline
3. Zhang, D.-W., Lagace, T. A., Garuti, R., Zhao, Z., McDonald, M., Horton, J. D., Cohen, J. C., and Hobbs, H. H. (2007) Binding of proprotein convertase subtilisin/kexin type 9 to epidermal growth factor-like repeat A of low density lipoprotein receptor decreases receptor recycling and increases degradation. *J. Biol. Chem.* **282,** 18602–18612 CrossRef Medline
4. Grefhorst, A., McNutt, M. C., Lagace, T. A., and Horton, J. D. (2008) Plasma PCSK9 preferentially reduces liver LDL receptors in mice. *J. Lipid Res.* **49,** 1303–1311 CrossRef Medline
5. Seidah, N. G. (2016) New developments in proprotein convertase subtilisin–kexin 9's biology and clinical implications. *Curr. Opin. Lipidol.* **27,** 274–281 CrossRef Medline

6. Cohen, J. C., Boerwinkle, E., Mosley, T. H., Jr., and Hobbs, H. H. (2006) Sequence variations in PCSK9, low LDL, and protection against coronary heart disease. *N. Engl. J. Med.* **354,** 1264–1272 CrossRef Medline
7. Ridker, P. M., Revkin, J., Amarenco, P., Brunell, R., Curto, M., Civeira, F., Flather, M., Glynn, R. J., Gregoire, J., Jukema, J. W., Karpov, Y., Kastelein, J. J. P., Koenig, W., Lorenzatti, A., Manga, P., *et al.* (2017) Cardiovascular Efficacy and Safety of Bococizumab in High-Risk Patients. *N. Engl. J. Med.* **376,** 1527–1539 CrossRef Medline
8. Sabatine, M. S., Giugliano, R. P., Keech, A. C., Honarpour, N., Wiviott, S. D., Murphy, S. A., Kuder, J. F., Wang, H., Liu, T., Wasserman, S. M., Sever, P. S., Pedersen, T. R., and FOURIER Steering Committee and Investigators (2017) Evolocumab and Clinical Outcomes in Patients with Cardiovascular Disease. *N. Engl. J. Med.* **376,** 1713–1722 CrossRef Medline
9. Maxwell, K. N., and Breslow, J. L. (2004) Adenoviral-mediated expression of Pcsk9 in mice results in a low-density lipoprotein receptor knockout phenotype. *Proc. Natl. Acad. Sci. U.S.A.* **101,** 7100–7105 CrossRef Medline
10. Naureckiene, S., Ma, L., Sreekumar, K., Purandare, U., Lo, C. F., Huang, Y., Chiang, L. W., Grenier, J. M., Ozenberger, B. A., Jacobsen, J. S., Kennedy, J. D., DiStefano, P. S., Wood, A., and Bingham, B. (2003) Functional characterization of Narc 1, a novel proteinase related to proteinase K. *Arch. Biochem. Biophys.* **420,** 55–67 CrossRef Medline
11. Seidah, N. G., and Prat, A. (2012) The biology and therapeutic targeting of the proprotein convertases. *Nat. Rev. Drug Discov.* **11,** 367–383 CrossRef Medline
12. Cunningham, D., Danley, D. E., Geoghegan, K. F., Griffor, M. C., Hawkins, J. L., Subashi, T. A., Varghese, A. H., Ammirati, M. J., Culp, J. S., Hoth, L. R., Mansour, M. N., McGrath, K. M., Seddon, A. P., Shenolikar, S., Stutzman-Engwall, K. J., Warren, L. C., Xia, D., and Qiu, X. (2007) Structural and biophysical studies of PCSK9 and its mutants linked to familial hypercholesterolemia. *Nat. Struct. Mol. Biol.* **14,** 413–419 CrossRef Medline
13. Mayne, J., Dewpura, T., Raymond, A., Bernier, L., Cousins, M., Ooi, T. C., Davignon, J., Seidah, N. G., Mbikay, M., and Chrétien, M. (2011) Novel loss-of-function PCSK9 variant is associated with low plasma LDL cholesterol in a French-Canadian family and with impaired processing and secretion in cell culture. *Clin. Chem.* **57,** 1415–1423 CrossRef Medline
14. Piper, D. E., Jackson, S., Liu, Q., Romanow, W. G., Shetterly, S., Thibault, S. T., Shan, B., and Walker, N. P. (2007) The crystal structure of PCSK9: a regulator of plasma LDL-cholesterol. *Structure* **15,** 545–552 CrossRef Medline
15. Hampton, E. N., Knuth, M. W., Li, J., Harris, J. L., Lesley, S. A., and Spraggon, G. (2007) The self-inhibited structure of full-length PCSK9 at 1.9 Å reveals structural homology with resistin within the C-terminal domain. *Proc. Natl. Acad. Sci. U.S.A.* **104,** 14604–14609 CrossRef Medline
16. Chorba, J. S., and Shokat, K. M. (2014) The proprotein convertase subtilisin/kexin type 9 (PCSK9) active site and cleavage sequence differentially regulate protein secretion from proteolysis. *J. Biol. Chem.* **289,** 29030–29043 CrossRef Medline
17. Hall, M. P., Unch, J., Binkowski, B. F., Valley, M. P., Butler, B. L., Wood, M. G., Otto, P., Zimmerman, K., Vidugiris, G., Machleidt, T., Robers, M. B., Benink, H. A., Eggers, C. T., Slater, M. R., Meisenheimer, P. L., *et al.* (2012) Engineered luciferase reporter from a deep sea shrimp utilizing a novel imidazopyrazinone substrate. *ACS Chem. Biol.* **7,** 1848–1857 CrossRef Medline
18. Benjannet, S., Rhainds, D., Hamelin, J., Nassoury, N., and Seidah, N. G. (2006) The proprotein convertase (PC) PCSK9 is inactivated by furin and/or PC5/6A: functional consequences of natural mutations and post-translational modifications. *J. Biol. Chem.* **281,** 30561–30572 CrossRef Medline
19. Zhao, Z., Tuakli-Wosornu, Y., Lagace, T. A., Kinch, L., Grishin, N. V., Horton, J. D., Cohen, J. C., and Hobbs, H. H. (2006) Molecular characterization of loss-of-function mutations in PCSK9 and identification of a compound heterozygote. *Am. J. Hum. Genet.* **79,** 514–523 CrossRef Medline
20. Kim, J. H., Lee, S.-R., Li, L.-H., Park, H.-J., Park, J.-H., Lee, K. Y., Kim, M.-K., Shin, B. A., and Choi, S.-Y. (2011) High cleavage efficiency of a 2A peptide derived from porcine teschovirus-1 in human cell lines, zebrafish and mice. *PLoS One* **6,** e18556 CrossRef Medline
21. Hasson, S. A., Fogel, A. I., Wang, C., MacArthur, R., Guha, R., Heman-Ackah, S., Martin, S., Youle, R. J., and Inglese, J. (2015) Chemogenomic profiling of endogenous PARK2 expression using a genome-edited coincidence reporter. *ACS Chem. Biol.* **10,** 1188–1197 CrossRef Medline
22. Benjannet, S., Rhainds, D., Essalmani, R., Mayne, J., Wickham, L., Jin, W., Asselin, M.-C., Hamelin, J., Varret, M., Allard, D., Trillard, M., Abifadel, M., Tebon, A., Attie, A. D., Rader, D. J., *et al.* (2004) NARC-1/PCSK9 and its natural mutants: zymogen cleavage and effects on the low density lipoprotein (LDL) receptor and LDL cholesterol. *J. Biol. Chem.* **279,** 48865–48875 CrossRef Medline
23. Engler, C., Kandzia, R., and Marillonnet, S. (2008) A one pot, one step, precision cloning method with high throughput capability. *PLoS One* **3,** e3647 CrossRef Medline
24. Cong, L., and Zhang, F. (2015) Genome engineering using CRISPR-Cas9 system. *Methods Mol. Biol.* **1239,** 197–217 CrossRef Medline
25. Benjannet, S., Hamelin, J., Chrétien, M., and Seidah, N. G. (2012) Loss- and gain-of-function Pcsk9 variants: cleavage specificity, dominant negative effects, and low density lipoprotein receptor (LDLR) degradation. *J. Biol. Chem.* **287,** 33745–33755 CrossRef Medline
26. Garvie, C. W., Fraley, C. V., Elowe, N. H., Culyba, E. K., Lemke, C. T., Hubbard, B. K., Kaushik, V. K., and Daniels, D. S. (2016) Point mutations at the catalytic site of PCSK9 inhibit folding, autoprocessing, and interaction with the LDL receptor. *Protein Sci.* **25,** 2018–2027 CrossRef Medline
27. Crooks, G. E., Hon, G., Chandonia, J.-M., and Brenner, S. E. (2004) WebLogo: a sequence logo generator. *Genome Res.* **14,** 1188–1190 CrossRef Medline
28. Cameron, J., Holla, Ø. L., Berge, K. E., Kulseth, M. A., Ranheim, T., Leren, T. P., and Laerdahl, J. K. (2008) Investigations on the evolutionary conservation of PCSK9 reveal a functionally important protrusion. *FEBS J.* **275,** 4121–4133 CrossRef Medline
29. Zhang, Y., Ultsch, M., Skelton, N. J., Burdick, D. J., Beresini, M. H., Li, W., Kong-Beltran, M., Peterson, A., Quinn, J., Chiu, C., Wu, Y., Shia, S., Moran, P., Di Lello, P., Eigenbrot, C., and Kirchhofer, D. (2017) Discovery of a cryptic peptide-binding site on PCSK9 and design of antagonists. *Nat. Struct. Mol. Biol.* **24,** 848–856 CrossRef Medline
30. McNutt, M. C., Lagace, T. A., and Horton, J. D. (2007) Catalytic activity is not required for secreted PCSK9 to reduce low density lipoprotein receptors in HepG2 cells. *J. Biol. Chem.* **282,** 20799–20803 CrossRef Medline
31. Cameron, J., Holla, Ø. L., Laerdahl, J. K., Kulseth, M. A., Berge, K. E., and Leren, T. P. (2009) Mutation S462P in the PCSK9 gene reduces secretion of mutant PCSK9 without affecting the autocatalytic cleavage. *Atherosclerosis* **203,** 161–165 CrossRef Medline
32. Leigh, S. E., Leren, T. P., and Humphries, S. E. (2009) Commentary PCSK9 variants: a new database. *Atherosclerosis* **203,** 32–33 CrossRef Medline
33. Landrum, M. J., Lee, J. M., Benson, M., Brown, G., Chao, C., Chitipiralla, S., Gu, B., Hart, J., Hoffman, D., Hoover, J., Jang, W., Katz, K., Ovetsky, M., Riley, G., Sethi, A., *et al.* (2016) ClinVar: public archive of interpretations of clinically relevant variants. *Nucleic Acids Res.* **44,** D862–D868 CrossRef Medline
34. Kwon, H. J., Lagace, T. A., McNutt, M. C., Horton, J. D., and Deisenhofer, J. (2008) Molecular basis for LDL receptor recognition by PCSK9. *Proc. Natl. Acad. Sci. U.S.A.* **105,** 1820–1825 CrossRef Medline
35. Cameron, J., Holla, Ø. L., Ranheim, T., Kulseth, M. A., Berge, K. E., and Leren, T. P. (2006) Effect of mutations in the PCSK9 gene on the cell surface LDL receptors. *Hum. Mol. Genet.* **15,** 1551–1558 CrossRef Medline
36. Cameron, J., Holla, O. L., Laerdahl, J. K., Kulseth, M. A., Ranheim, T., Rognes, T., Berge, K. E., and Leren, T. P. (2008) Characterization of novel mutations in the catalytic domain of the PCSK9 gene. *J. Intern. Med.* **263,** 420–431 CrossRef Medline
37. McNutt, M. C., Kwon, H. J., Chen, C., Chen, J. R., Horton, J. D., and Lagace, T. A. (2009) Antagonism of secreted PCSK9 increases low density lipoprotein receptor expression in HepG2 cells. *J. Biol. Chem.* **284,** 10561–10570 CrossRef Medline
38. Homer, V. M., Marais, A. D., Charlton, F., Laurie, A. D., Hurndell, N., Scott, R., Mangili, F., Sullivan, D. R., Barter, P. J., Rye, K.-A., George, P. M.,

and Lambert, G. (2008) Identification and characterization of two non-secreted PCSK9 mutants associated with familial hypercholesterolemia in cohorts from New Zealand and South Africa. *Atherosclerosis* **196,** 659–666 CrossRef Medline

39. Du, F., Hui, Y., Zhang, M., Linton, M. F., Fazio, S., and Fan, D. (2011) Novel domain interaction regulates secretion of proprotein convertase subtilisin/kexin type 9 (PCSK9) protein. *J. Biol. Chem.* **286,** 43054–43061 CrossRef Medline
40. Niers, J. M., Kerami, M., Pike, L., Lewandrowski, G., and Tannous, B. A. (2011) Multimodal *in vivo* imaging and blood monitoring of intrinsic and extrinsic apoptosis. *Mol. Ther.* **19,** 1090–1096 CrossRef Medline
41. Ketteler, R., Sun, Z., Kovacs, K. F., He, W.-W., and Seed, B. (2008) A pathway sensor for genome-wide screens of intracellular proteolytic cleavage. *Genome Biol.* **9,** R64 CrossRef Medline
42. Qu, L., Vongpunsawad, S., Atmar, R. L., Prasad, B. V. V., and Estes, M. K. (2014) Development of a Gaussia luciferase-based human norovirus protease reporter system: cell type-specific profile of Norwalk virus protease precursors and evaluation of inhibitors. *J. Virol.* **88,** 10312–10326 CrossRef Medline
43. Bartok, E., Bauernfeind, F., Khaminets, M. G., Jakobs, C., Monks, B., Fitzgerald, K. A., Latz, E., and Hornung, V. (2013) iGLuc: a luciferase-based inflammasome and protease activity reporter. *Nat. Methods* **10,** 147–154 CrossRef Medline
44. Miyake, Y., Kimura, R., Kokubo, Y., Okayama, A., Tomoike, H., Yamamura, T., and Miyata, T. (2008) Genetic variants in PCSK9 in the Japanese population: rare genetic variants in PCSK9 might collectively contribute to plasma LDL cholesterol levels in the general population. *Atherosclerosis* **196,** 29–36 CrossRef Medline
45. Lakoski, S. G., Lagace, T. A., Cohen, J. C., Horton, J. D., and Hobbs, H. H. (2009) Genetic and metabolic determinants of plasma PCSK9 levels. *J. Clin. Endocrinol. Metab.* **94,** 2537–2543 CrossRef Medline
46. Dubuc, G., Tremblay, M., Paré, G., Jacques, H., Hamelin, J., Benjannet, S., Boulet, L., Genest, J., Bernier, L., Seidah, N. G., and Davignon, J. (2010) A new method for measurement of total plasma PCSK9: clinical applications. *J. Lipid Res.* **51,** 140–149 CrossRef Medline
47. Wanneh, E., Luna, G., Dufour, R., and Baass, A. (2017) Predicting proprotein convertase subtilisin kexin type-9 loss of function mutations using plasma PCSK9 concentration. *J. Clin. Lipidol.* **11,** 55–60 CrossRef Medline
48. Persson, L., Cao, G., Ståhle, L., Sjöberg, B. G., Troutt, J. S., Konrad, R. J., Gälman, C., Wallén, H., Eriksson, M., Hafström, I., Lind, S., Dahlin, M., Amark, P., Angelin, B., and Rudling, M. (2010) Circulating proprotein convertase subtilisin kexin type 9 has a diurnal rhythm synchronous with cholesterol synthesis and is reduced by fasting in humans. *Arterioscler. Thromb. Vasc. Biol.* **30,** 2666–2672 CrossRef Medline
49. Cariou, B., Langhi, C., Le Bras, M., Bortolotti, M., Lê, K.-A., Theytaz, F., Le May, C., Guyomarc'h-Delasalle, B., Zaïr, Y., Kreis, R., Boesch, C., Krempf, M., Tappy, L., and Costet, P. (2013) Plasma PCSK9 concentrations during an oral fat load and after short term high-fat, high-fat high-protein and high-fructose diets. *Nutr. Metab.* (*Lond.*) **10,** 4 CrossRef Medline
50. Browning, J. D., and Horton, J. D. (2010) Fasting reduces plasma proprotein convertase, subtilisin/kexin type 9 and cholesterol biosynthesis in humans. *J. Lipid Res.* **51,** 3359–3363 CrossRef Medline
51. Lagace, T. A., Curtis, D. E., Garuti, R., McNutt, M. C., Park, S. W., Prather, H. B., Anderson, N. N., Ho, Y. K., Hammer, R. E., and Horton, J. D. (2006) Secreted PCSK9 decreases the number of LDL receptors in hepatocytes and in livers of parabiotic mice. *J. Clin. Invest.* **116,** 2995–3005 CrossRef Medline
52. Essalmani, R., Susan-Resiga, D., Chamberland, A., Abifadel, M., Creemers, J. W., Boileau, C., Seidah, N. G., and Prat, A. (2011) *In vivo* evidence that furin from hepatocytes inactivates PCSK9. *J. Biol. Chem.* **286,** 4257–4263 CrossRef Medline
53. Ai, X., Palyha, O. C., Ha, S., Quan, S., Chu, D., Zhang, A., Wisniewski, D., Fischer, P., Painter, R., Xiao, J., Ichetovkin, M., Baysarowich, J., Szeto, D., Rosenbach, M., Ni, W., Xie, D., *et al.* (2016) C-terminal loop mutations determine folding and secretion properties of PCSK9. *Biochem. Mol. Biol. J.* **2,** 17 CrossRef
54. Horton, J. D., Shah, N. A., Warrington, J. A., Anderson, N. N., Park, S. W., Brown, M. S., and Goldstein, J. L. (2003) Combined analysis of oligonucleotide microarray data from transgenic and knockout mice identifies direct SREBP target genes. *Proc. Natl. Acad. Sci. U.S.A.* **100,** 12027–12032 CrossRef Medline
55. Dubuc, G., Chamberland, A., Wassef, H., Davignon, J., Seidah, N. G., Bernier, L., and Prat, A. (2004) Statins upregulate PCSK9, the gene encoding the proprotein convertase neural apoptosis-regulated convertase-1 implicated in familial hypercholesterolemia. *Arterioscler. Thromb. Vasc. Biol.* **24,** 1454–1459 CrossRef Medline
56. Lochhead, P. A., Sibbet, G., Morrice, N., and Cleghon, V. (2005) Activation-loop autophosphorylation is mediated by a novel transitional intermediate form of DYRKs. *Cell* **121,** 925–936 CrossRef Medline
57. Foote, J., Lauritzen, A. M., and Lipscomb, W. N. (1985) Substrate specificity of aspartate transcarbamylase: interaction of the enzyme with analogs of aspartate and succinate. *J. Biol. Chem.* **260,** 9624–9629 Medline
58. Joshi, N., Hoobler, E. K., Perry, S., Diaz, G., Fox, B., and Holman, T. R. (2013) Kinetic and structural investigations into the allosteric and pH effect on the substrate specificity of human epithelial 15-lipoxygenase-2. *Biochemistry* **52,** 8026–8035 CrossRef Medline
59. Shelton, C. C., Zhu, L., Chau, D., Yang, L., Wang, R., Djaballah, H., Zheng, H., and Li, Y.-M. (2009) Modulation of γ-secretase specificity using small molecule allosteric inhibitors. *Proc. Natl. Acad. Sci. U.S.A.* **106,** 20228–20233 CrossRef Medline
60. Gibson, D. G., Young, L., Chuang, R.-Y., Venter, J. C., Hutchison, C. A., 3rd, and Smith, H. O. (2009) Enzymatic assembly of DNA molecules up to several hundred kilobases. *Nat. Methods* **6,** 343–345 CrossRef Medline
61. Liu, H., and Naismith, J. H. (2008) An efficient one-step site-directed deletion, insertion, single and multiple-site plasmid mutagenesis protocol. *BMC Biotechnol.* **8,** 91 CrossRef Medline
62. Zhang, J. H., Chung, T. D., and Oldenburg, K. R. (1999) A simple statistical parameter for use in evaluation and validation of high throughput screening assays. *J. Biomol. Screen.* **4,** 67–73 CrossRef Medline
63. Fiser, A., and Sali, A. (2003) ModLoop: automated modeling of loops in protein structures. *Bioinformatics* **19,** 2500–2501 CrossRef Medline